Monthly Notices
of the
ROYAL ASTRONOMICAL SOCIETY

MNRAS **444,** 3488–3500 (2014) doi:10.1093/mnras/stu1698

Dynamical tides in compact white dwarf binaries: influence of rotation

Jim Fuller[1,2]★ and Dong Lai[3]★

[1]*TAPIR, Mailcode 350-17, California Institute of Technology, Pasadena, CA 91125, USA*
[2]*Kavli Institute for Theoretical Physics, Kohn Hall, University of California, Santa Barbara, CA 93106, USA*
[3]*Center for Space Research, Department of Astronomy, Cornell University, Ithaca, NY 14853, USA*

Accepted 2014 August 18. Received 2014 July 24; in original form 2014 June 10

ABSTRACT

Tidal interactions play an important role in the evolution and ultimate fate of compact white dwarf (WD) binaries. Not only do tides affect the pre-merger state (such as temperature and rotation rate) of the WDs, but they may also determine which systems merge and which undergo stable mass transfer. In this paper, we attempt to quantify the effects of rotation on tidal angular momentum transport in binary stars, with specific calculations applied to WD stellar models. We incorporate the effect of rotation using the traditional approximation, in which the dynamically excited gravity waves within the WDs are transformed into gravitoinertial Hough waves. The Coriolis force has only a minor effect on prograde gravity waves, and previous results predicting the tidal spin-up and heating of inspiraling WDs are not significantly modified. However, rotation strongly alters retrograde gravity waves and inertial waves, with important consequences for the tidal spin-down of accreting WDs. We identify new dynamical tidal forcing terms that arise from a proper separation of the equilibrium and dynamical tide components; these new forcing terms are very important for systems near synchronous rotation. Additionally, we discuss the impact of Stokes drift currents on the wave angular momentum flux. Finally, we speculate on how tidal interactions will affect supersynchronously rotating WDs in accreting systems.

Key words: hydrodynamics – waves – binaries *(including multiple)*: close – stars: oscillations *(including pulsations)* – white dwarfs.

1 INTRODUCTION

Merging and mass-transferring white dwarfs (WDs) are responsible for the creation of a variety of exotic astrophysical systems and events. Among these are isolated sdB/sdO stars (likely created by the merger of two He WDs; Saio & Jeffery 2000; Han et al. 2002; Heber 2009), R CrB stars (likely created by the merger of a CO and He WD; Webbink 1984; Iben, Tutukov & Yungelson 1996; Jeffery, Karakas & Saio 2011; Clayton 2012), AM CVn binaries (possibly created by stable mass transfer from a He WD on to a CO WD; Warner 1995; Tutukov & Yungelson 1996; Han & Webbink 1999; Nelemans et al. 2001b), and possibly high-mass neutron stars and magnetars (created by the accretion-induced collapse of merging CO WDs or accreting O–Ne–Mg WDs; Saio & Nomoto 1985; Nomoto & Kondo 1991; Saio & Nomoto 2004). More importantly, merging or accreting CO WDs may be the progenitors of Type Ia supernovae (Iben & Tutukov 1984; Webbink 1984, Di Stefano 2010; Gilfanov & Bogdan 2010; Maoz, Sharon & Gal-Yam 2010; Li et al. 2011; Bloom et al. 2012; Gonzalez Hernandez et al. 2012; Schaefer & Pagnotta 2012), although the pre-supernova conditions of the WD are still a subject of intense investigation.

★E-mail: jfuller@caltech.edu (JF); dong@astro.cornell.edu (DL)

Compact WD binaries (with periods in the range of minutes to hours) are also being discovered at an accelerating pace (e.g. Mullally et al. 2009; Kulkarni & van Kerkwijk 2010; Steinfadt et al. 2010; Brown et al. 2012; Kilic et al. 2012, 2013, see Marsh 2011 for a review). These systems will begin mass transfer within a Hubble time, although it is not always clear which observed WD systems will result in which phenomena. Recent simulations (e.g. Segretain, Chabrier & Mochkovitch 1997; Yoon, Podsiadlowski & Rosswog 2007; Loren-Aguilar, Isern & Garcia-Berro 2009; van Kerkwijk, Chang & Justham 2010; Dan et al. 2012, 2013; Raskin et al. 2012) have shed new light on the outcome of WD mergers. However, the initial conditions of these simulations are predicated upon the tidal effects that precede (and may ultimately determine the stability of) the mass-transfer process. It is thus crucial to understand how tides operate up to the moment of Roche lobe overflow.

It is also important to quantify the rate of tidal dissipation once mass transfer begins. Previous works (Nelemans, Steeghs & Groot 2001a; Marsh, Nelemans & Steeghs 2004) have shown that the strength of tidal torques may be important in determining the stability of mass transfer. Low-mass ratio systems with $M_2/M_1 \lesssim 1/4$ are expected to have stable mass transfer, while high-mass ratio systems with $M_2/M_1 \gtrsim 2/3$ are expected to be unstable and merge. The fates of intermediate mass ratio systems with $M_2/M_1 \sim 1/2$ (such as the recently discovered 12.75 min binary, Brown et al. 2011) are less

certain. The stability of mass transfer in these systems may depend on the rate at which tidal torques can transfer rotational angular momentum from the accretor back to the orbit.

This paper is the fifth in a series (see Fuller & Lai 2011, 2012a,b, 2013, hereafter Papers I–IV, respectively) dedicated to the physics of tidal interactions and their observational consequences in compact WD binaries. In these previous works, we examined the tidal excitation, propagation, and dissipation of gravity waves (g-waves) that are restored by buoyancy forces within CO and He WDs. The waves dissipate energy and angular momentum, leading to the rotational synchronization and tidal heating of WDs prior to merger or mass transfer. We found that gravity waves are excited at compositional gradients within the WDs and propagate towards the surface where they become highly non-linear, causing them to break and locally deposit their angular momentum. This results in strong tidal heating in the outer layers of the WD, and causes the WDs to be spun up from the outside in.

Tides in WDs have also been examined in several previous works using parametrized tidal dissipation laws (Iben, Tutukov & Fedorova 1998; Piro 2011; Dall'Osso & Rossi 2013) and in calculations of the tidal excitation of oscillation modes (Willems, Deloye & Kalogera 2010; Valsecchi et al. 2012). However, for the short orbital periods at which tidal effects are most important, it is the continuous excitation of outgoing gravity waves, rather than excitation of discrete g modes (Fuller & Lai 2011), that dominates the tidal dissipation in WD binaries. Encouragingly, the detailed study of WD tides by Burkart et al. (2013) utilizes techniques comparable to Papers I and II, and reaches generally similar conclusions.

The studies listed above (and all previous works that we know of) have ignored the influence of rotation on the wave dynamics. While this approximation works for slowly spinning WDs at the beginning of the tidal spin-up process, it breaks down for WDs nearing synchronous rotation in which the tidal forcing frequency becomes comparable to the spin frequency. The approximation is even worse for WDs being spun up to supersynchronous rotation via mass transfer.

In this study, we attempt to quantify the effect of the Coriolis force on the efficiency of tidal angular momentum transport. To do this, we employ the so-called traditional approximation frequently used to study the influence of rotation on gravity waves (see e.g. Chapman & Lindzen 1970; Bildsten et al. 1996; Lee & Saio 1997; Townsend 2003). The Coriolis force modifies the angular dependence of the gravity waves, confining them to the equatorial region of the star. This affects their overlap with the (predominantly quadrupolar) tidal potential that excites them. Moreover, the Coriolis force modifies the radial wavelength of gravity waves, which in turn affects the amplitude to which they are excited. Finally, the Coriolis force allows for the existence of inertial and Rossby waves (r-waves), which are especially important in supersynchronously rotating WDs in which tidal dissipation occurs through the excitation of retrograde waves (i.e. the wave pattern propagates opposite to the direction of the spin in a frame corotating with the WD).

This paper is organized as follows. In Section 2, we review the influence of rotation under the traditional approximation, and we examine its effect on tidally excited gravitoinertial waves. In Section 3, we investigate the effects of rotation on the excitation of the dynamical tide and discuss how the dynamical tide transports energy angular momentum. In Section 4, we present our numerical results of tidal dissipation rates in rotating WDs and analyse its effect on the orbital and spin evolution of compact WD binaries. Finally, in Section 5, we discuss the implications of our results, and how they may affect WDs in various types of compact binary systems.

2 INFLUENCE OF ROTATION IN THE TRADITIONAL APPROXIMATION

The influence rotation on stellar oscillations has been examined in many previous works, and we choose to follow along the lines of Bildsten et al. (1996) and Lee & Saio (1997) (although note the sign difference in their definition of ω and m). Here we review the basic physics in order to understand how rotation will affect tidally excited waves in WDs. The perturbed linearized momentum equation in the rotating frame of a spherical star may be written as

$$-\rho\omega^2\boldsymbol{\xi} = -\nabla\delta P - \rho\nabla U - g\delta\rho\hat{\boldsymbol{r}} + 2\mathrm{i}\rho\omega\boldsymbol{\Omega}_\mathrm{s}\times\boldsymbol{\xi}. \tag{1}$$

Here, $\boldsymbol{\xi}$ is the Lagrangian displacement vector, δP is the Eulerian pressure perturbation, $\boldsymbol{\Omega}_\mathrm{s}$ is the star's spin vector, U is the tidal potential of the companion star, and the other quantities have their usual meaning. We have assumed a time dependence $\boldsymbol{\xi}\propto \mathrm{e}^{-\mathrm{i}\omega t}$, and we have adopted the Cowling approximation (i.e. we have ignored the perturbation to the star's gravitational potential, which is a good approximation for the gravity waves of interest). Additionally, we have ignored the centrifugal force and stellar oblateness, which is a good approximation as long as the stellar spin is much smaller than breakup, i.e. when $\Omega_\mathrm{s}\ll\Omega_\mathrm{dyn}=\sqrt{GM/R^3}$. Finally, we assume that the star rotates rigidly along the z-axis such that $\boldsymbol{\Omega}_\mathrm{s}=\Omega_\mathrm{s}\hat{\boldsymbol{z}}$, with the spin vector aligned with the orbital angular momentum.

For adiabatic oscillations, the perturbed momentum equations become

$$-\rho\omega^2\xi_r = -\frac{\partial}{\partial r}(\delta P+\rho U)+U\frac{\partial\rho}{\partial r}-\frac{g}{c_\mathrm{s}^2}\delta P - \rho N^2\xi_r - 2\mathrm{i}\Omega_\mathrm{s}\omega\rho\xi_\phi\sin\theta, \tag{2}$$

$$-\rho\omega^2\xi_\theta = -\frac{1}{r}\frac{\partial}{\partial\theta}(\delta P+\rho U) - 2\mathrm{i}\Omega_\mathrm{s}\omega\rho\xi_\phi\cos\theta, \tag{3}$$

$$-\rho\omega^2\xi_\phi = -\frac{1}{r\sin\theta}\frac{\partial}{\partial\phi}(\delta P+\rho U) + 2\mathrm{i}\Omega_\mathrm{s}\omega\rho\left(\xi_\theta\cos\theta+\xi_r\sin\theta\right). \tag{4}$$

Here, we have used the adiabatic relation

$$\delta\rho = \frac{1}{c_\mathrm{s}^2}\delta P + \frac{\rho N^2}{g}\xi_r, \tag{5}$$

where c_s is the sound speed and N is the Brunt–Vaisala frequency. Additionally, the continuity equation implies

$$\delta\rho + \frac{1}{r^2}\frac{\partial}{\partial r}\left(\rho r^2\xi_r\right) + \rho\nabla_\perp\cdot\boldsymbol{\xi}_\perp = 0, \tag{6}$$

where the subscript $\perp$ denotes the horizontal part of each vector.

In the traditional approximation, the last term in equations (2) and (4) are ignored. The traditional approximation works well for gravity waves, which in the non-rotating WKB limit (and with l and m of order unity) have $\xi_\theta\sim\xi_\phi\sim(N/\omega)\xi_r$. Then, in regions in the star where $N\gg\omega$, the last terms in equations (2) and (4) become negligible and may be discarded. Equation (2) then separates from equations (3) and (4), and the angular dependence of the waves separates from the radial dependence.

The traditional approximation will be valid for the dynamical tide of a rotating WD, which is comprised mainly of rotationally

modified gravitoinertial waves in the outer layers of the star (see Paper II). In both the region of wave excitation (at composition gradients within the WD) and the outer boundary (in the hydrogen atmosphere of the WD), we find $N \gg \omega$ and $\xi_\perp \gg \xi_r$, so the traditional approximation is valid. Near the centre of the star, the traditional approximation breaks down because $N \to 0$. Therefore, our calculations will not accurately characterize the dynamical tide in this region. However, we find this region has very little effect on the dynamical tide in the outer layers of the star (see Appendix C), and does not significantly alter the torques calculated in Section 4.

In contrast to the dynamical tide, the traditional approximation does not apply to the equilibrium tide, which is the hydrostatic response of the star to the tidal potential. To circumvent this problem, we decompose the response of the star into equilibrium and dynamical components:

$$\boldsymbol{\xi} = \boldsymbol{\xi}^{\rm eq} + \boldsymbol{\xi}^{\rm dyn}. \tag{7}$$

We solve for the equilibrium tide $\boldsymbol{\xi}^{\rm eq}$ and subtract it from equations (2)–(6), so that we can solve for $\boldsymbol{\xi}^{\rm dyn}$ using the traditional approximation. We detail this procedure in Appendix A.

2.1 Hough functions

The angular dependence of $\boldsymbol{\xi}^{\rm dyn}$ is found by solving Laplace's tidal equation

$$\mathcal{L}(H_k) = -\lambda_k H_k, \tag{8}$$

where λ_k is an angular eigenvalue, H_k is its associated eigenfunction (the Hough function), and the operator $\mathcal{L}$ is

$$\mathcal{L} = \frac{\partial}{\partial\mu}\left(\frac{1-\mu^2}{1-q^2\mu^2}\frac{\partial}{\partial\mu}\right) - \frac{m^2}{(1-\mu^2)(1-q^2\mu^2)} + \frac{qm(1+q^2\mu^2)}{(1-q^2\mu^2)^2}. \tag{9}$$

Here, $\mu = \cos\theta$ and m is the azimuthal number of the wave such that $\boldsymbol{\xi} \propto {\rm e}^{{\rm i}m\phi}$. In this convention, prograde waves (in the rotating frame) have $m > 0$ and retrograde waves have $m < 0$. The parameter q that determines the behaviour of the Hough functions is defined as

$$q = \frac{2\Omega_{\rm s}}{\omega}. \tag{10}$$

Rotation becomes important for $q \gtrsim 1$, and it is easily verified that the solutions to equation (8) converge to the associated Legendre polynomials as $q \to 0$.

As discussed in Lee & Saio (1997), the angular dependence of the perturbed variables in the traditional approximation is

$$\xi_r(r,\theta,\phi,t) = \xi_r(r) H_k(\mu) {\rm e}^{{\rm i}m\phi - {\rm i}\omega t}, \tag{11}$$

whereas

$$\xi_\theta(r,\theta,\phi,t) = \xi_\perp(r)\frac{1}{(1-\mu^2q^2)\sqrt{1-\mu^2}} \times \left[-mq\mu - (1-\mu^2)\frac{\partial}{\partial\mu}\right] H_k(\mu){\rm e}^{{\rm i}m\phi-{\rm i}\omega t}, \tag{12}$$

and

$$\xi_\phi(r,\theta,\phi,t) = \xi_\perp(r)\frac{i}{(1-\mu^2q^2)\sqrt{1-\mu^2}} \times \left[m + q\mu(1-\mu^2)\frac{\partial}{\partial\mu}\right] H_k(\mu){\rm e}^{{\rm i}m\phi-{\rm i}\omega t}. \tag{13}$$

Here, $\xi_\perp(r) \equiv \delta P(r)/(\rho r\omega^2)$. We have adopted the indexing notation of Lee & Saio (1997) to identify the Hough functions. The k subscript specifies the branch on which the Hough function lies, and (for $k \geq 0$) indicates the number of nodes in the angular eigenfunction in the non-rotating ($q \to 0$) limit. Thus, the $k = 0$ modes correspond to $l = |m|$ modes, $k = 1$ corresponds to $l = |m| + 1$, etc.

For $q < 1$, equation (8) is a Sturm–Liouville problem, and each solution can be traced back to an associated Legendre polynomial at $q = 0$. For $q > 1$, equation (8) is no longer a Sturm–Liouville problem, and additional solutions exist. These solutions correspond to r modes and inertial modes, which only exist in the range $\omega < 2\Omega_{\rm s}$, i.e. $q > 1$. Lee & Saio (1997) label these solutions with negative values of k, and we adopt the same convention here. However, we note that the $k = -2$ r mode has no nodes in its angular eigenfunction, similar to the $k = 0$ mode. For this reason, it will be the most important retrograde mode in tidal processes for $q \gg 1$.

We solve equation (8) for $m = \pm 2$ in the range $10^{-2} < q < 10^2$ using relaxation techniques. This method avoids many of the problems associated with singularities discussed by Bildsten et al. (1996) and Lee & Saio (1997). We normalize the Hough functions in the same manner as spherical harmonics:

$$\int {\rm d}A\, |H_k(\mu)|^2 = 1, \tag{14}$$

with the integral extending over the surface of a sphere, $\int {\rm d}A = 2\pi\int_{-1}^{1}{\rm d}\mu$. We limit our analysis to $m = \pm 2$ waves because they couple most strongly to the tidal potential, which is dominated by $l = |m| = 2$ components.

Fig. 1 shows a plot of the eigenvalues λ_k for the $k = 0$ and $k = -2$ branches.[1] For $q \ll 1$, the $k = 0$ solutions converge to $\lambda_k = |m|(|m| + 1)$, as expected. For $q \gg 1$, the $m = 2$, $k = 0$ solution asymptotes to $\lambda_k = m^2$ while the $m = -2$ mode increases proportional to q^2 as discussed in Bildsten et al. (1996). As q increases, the eigenfunctions H_k become localized near the equator, especially for the $m = -2$ solution.

The $k = -2$ solutions emerge for $q > 1$. Their eigenvalues λ_k asymptote to negative infinity at $q = 1$ and become positive at $q = (|m| + |k|)(|m| + |k + 1|)/|m| = 6$ for $m = -2$, $k = -2$. The value of λ_k remains below zero at all values of q for $m = 2$, $k < 0$ modes. Physically, this is significant because waves in the WKB limit follow the dispersion relation

$$k_r^2 = \frac{(L_k^2 - \omega^2)(N^2 - \omega^2)}{\omega^2 c_{\rm s}^2}, \tag{15}$$

where k_r is the radial wavenumber and

$$L_k^2 = \frac{\lambda_k c_{\rm s}^2}{r^2} \tag{16}$$

is the Lamb frequency squared. If $\lambda_k < 0$, gravity waves are evanescent where $\omega^2 < N^2$. Instead, these waves propagate as inertial

[1] Odd values of k are antisymmetric about the equator and cannot be excited by a circular, aligned orbit. The $k > 0$ branches couple most strongly with the $l > 2$ components of the tidal potential, which are small and can be ignored.

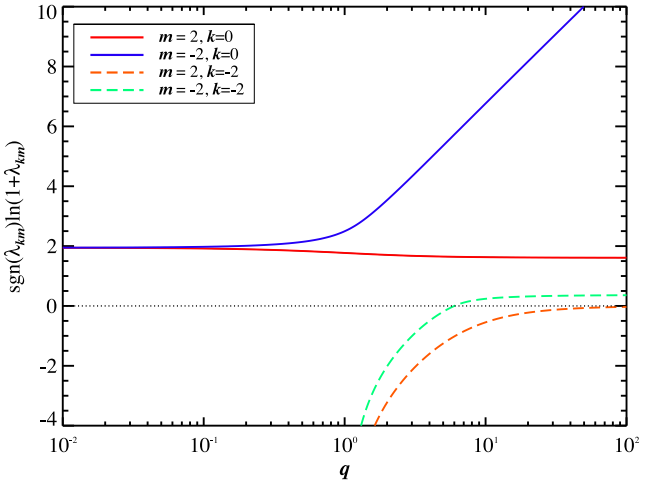

Figure 1. Eigenvalue λ_k of equation (8) as a function of the spin parameter $q = 2\Omega_s/\omega$, for a few different branches of solutions relevant to tidal dynamics. For comparison, we construct this plot in a similar fashion to fig. 1 of Lee & Saio (1997). The horizontal dashed line denotes $\lambda_k = 0$, below which the traditional approximation breaks down in the bulk of the radiative interior of a WD.

waves in regions where $\omega^2 > N^2$. We do not examine these inertial waves in detail because they do not satisfy the assumptions of the traditional approximation. However, the $m = -2$, $k = -2$ waves with $\lambda_k > 0$ behave like gravity waves where $\omega^2 \ll N^2$. We refer to them as r-waves. The r-waves satisfy the assumptions of the traditional approximation and can be accurately characterized by our techniques.

3 TIDAL RESPONSE IN ROTATING WHITE DWARFS

3.1 Response to tidal forcing

The extent to which an angular mode contributes to tidal processes is largely determined by its overlap with the tidal potential, which can be expanded in spherical harmonics. In the rotating frame of the stars, the largest time-variable components are the $l = |m| = 2$ components:

$$U_{2,m}(\boldsymbol{r}, t) + U_{2,-m}(\boldsymbol{r}, t) = U(r)\left[Y_{2m}(\theta, \phi)\mathrm{e}^{-\mathrm{i}\omega t} + Y^*_{2m}(\theta, \phi)\mathrm{e}^{\mathrm{i}\omega t}\right] \tag{17}$$

with

$$U(r) = -\frac{GM'W_{22}}{a^3}r^2 \tag{18}$$

and

$$\omega = m(\Omega - \Omega_s), \tag{19}$$

with Ω being the orbital frequency of the binary, a the semimajor axis, and $W_{22} = \sqrt{3\pi/10}$. In the preceding (and following) sections we have chosen to work with the $\mathrm{e}^{-\mathrm{i}\omega t}$ term with $\omega > 0$. Therefore, when $\Omega > \Omega_s$, we use $m = 2$ such that the orbit is prograde, and when $\Omega < \Omega_s$ we use $m = -2$ such that orbit is retrograde (in the rotating frame of the star).

The tidal potential appears as a forcing term in equations (2)–(4), but as noted above (see also Paper II), we must subtract out the equilibrium tidal response to solve for the dynamical tide. The forced oscillation equations for the dynamical part of the tidal response are (see Appendix A)

$$\frac{\partial}{\partial r}\delta P^{\rm dyn} = -\frac{g}{c_s^2}\delta P^{\rm dyn} + \rho\left(\omega^2 - N^2\right)\xi_r^{\rm dyn} + h_{klm}\rho\omega^2\xi_r^{\rm eq} + h_{klm}mq\rho\omega^2\xi_\perp^{\rm eq}, \tag{20}$$

$$\frac{\partial}{\partial r}\xi_r^{\rm dyn} = \left(\frac{g}{c_s^2} - \frac{2}{r}\right)\xi_r^{\rm dyn} + \left(\frac{\lambda_k}{\rho r^2\omega^2} - \frac{1}{\rho c_s^2}\right)\delta P^{\rm dyn} - \frac{h_{klm}l(l+1)}{r}\xi_\perp^{\rm eq} - \frac{g_{klm}}{r}\xi_r^{\rm eq}. \tag{21}$$

These equations describe the forced response of a Hough wave (specified by indices k and m) due to one component of the tidal potential (specified by indices l and m). All quantities are functions of r only, as we have already integrated over their angular dependence.

The key observation used to derive equations (20) and (21) is that the traditional approximation applies to the dynamical tide *but not to the equilibrium tide*. Properly subtracting the equilibrium tide leads to the appearance of the last terms in equations (20) and (21), which are additional forcing terms due to the Coriolis force on the equilibrium tide. These terms vanish in the non-rotating ($q \to 0$) limit but are very important when $q \gg 1$.[2]

The coefficients h_{klm} and g_{klm} are angular overlap integrals between Hough functions and spherical harmonics, and are given by equations (A17) and (A18) in Appendix A. The Hough functions form a complete basis, so to calculate the full tidal response one must project the tidal response on to every Hough function H_k. In practice, the tidal torque is dominated by the lowest order Hough functions, i.e. the Hough functions with the smallest values of $|\lambda_k|$, indexed by $k = 0$ and $k = -2$. We therefore focus only on the tidal response due to the $k = 0$ and -2 Hough waves.

Fig. 2 shows values of h_{klm} and g_{klm} as a function of q for the $l = |m| = 2$ component of the tidal potential. In the non-rotating limit $q \to 0$, the Hough functions reduce to spherical harmonics, $h_{klm} \to \delta_{k,\,l\,-\,m}$, and $g_{klm} \to 0$. For $k = 0$ waves, the value of h_{k2m} falls off monotonically with increasing q. For the prograde $m = 2$ waves, h_{k2m} falls off slowly, and the $k = 0$, $m = 2$ gravity waves dominate the tidal energy transfer at all values of q for subsyncronous rotation ($\Omega > \Omega_s$). However, h_{k2m} falls off much more rapidly for the $m = -2$ waves, diminishing their impact on tidal energy transfer. Instead, the $k = -2$ waves become important, with the value of h_{k2m} approaching unity for $q \approx 20$, and slowly decreasing for larger values of q. Therefore, while the $k = 0, m = -2$ gravity waves are most important at low values of q for supersynchronous rotation ($\Omega < \Omega_s$), the $k = -2$, $m = -2$ r-waves become important for $q \gtrsim 6$.[3]

For $q \gg 1$, we find $g_{k2m} \gg 1$ for all branches of Hough waves considered here. From Fig. 2, it is evident that when $q \gg 1$, $g_{klm} \propto q$ for the $k = 0$, $m = 2$ branch and the $k = -2$, $m = -2$ branch, whereas $g_{klm} \propto q^2$ for the $k = 0$, $m = -2$ branch (although we shall see below that this branch contributes negligibly to tidal torque in

[2] Ogilvie & Lin 2004 also comment on the necessary separation between the equilibrium tide and the dynamical tide. In their methods, they do not explicitly examine the additional forcing terms in equations (20) and (21), although they do note that the dynamical tide is essentially forced by the equilibrium tide rather than the tidal potential.

[3] For $1 \lesssim q \lesssim 6$, the traditional approximation does not accurately characterize the $k = -2$, $m = -2$ r-waves. It remains unclear whether the $k = -2$ branch of waves can contribute significantly to tidal dissipation in this range of q.

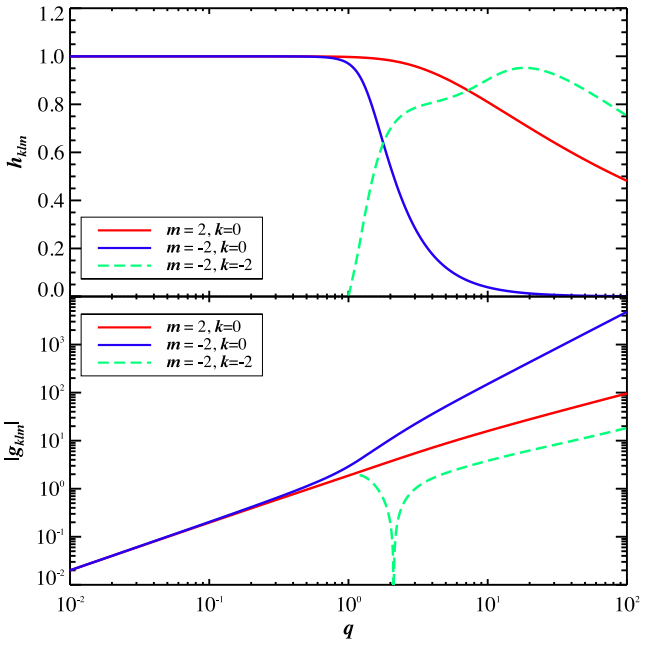

Figure 2. Angular overlap integrals h_{klm} and $|g_{klm}|$ (defined in equations A17 and A18) with the $l = 2$ component of the tidal potential as a function of q. The $k = -2$ r-wave solution does not exist for $q < 1$.

WDs when $q \gg 1$). Thus, the g_{k2m} term can dominate the tidal forcing for large values of q, and the failure to include it may lead to large errors in the calculation of the dynamical tidal response.

3.2 Angular momentum transport

The tidally excited waves carry energy and angular momentum from the region of excitation to the region of wave damping. As in Papers II–IV, we assume that the waves propagate into the outer layers of the star, depositing their energy and angular momentum in the low density subsurface regions where the waves become highly non-linear and break (we justify this assumption in Section 4, but see Papers II and IV for more discussion on non-linear wave breaking). Consequently, we impose a radiative outer boundary condition[4] as described in Paper II. The net tidal torque on the star is then calculated from the angular momentum luminosity flowing through the outer boundary.

The z-component of the wave angular momentum flux through a spherical surface at radius r is

$$\begin{aligned}\dot{J}_z(r) &= \left\langle r^2 \int \mathrm{d}A \xi_r(r,\theta,\phi,t) \frac{\partial}{\partial \phi} \right. \\ &\quad \left. \times (\delta P(r,\theta,\phi,t) + \rho U(r,\theta,\phi,t)) \right\rangle + cc \\ &= 2r^2 \int \mathrm{d}A \mathrm{Re}\left[\xi_r^*(r,\theta,\phi) \frac{\partial}{\partial \phi} \right. \\ &\quad \left. \times (\delta P(r,\theta,\phi) + \rho U(r,\theta,\phi)) \right] \\ &= 2mr^2 \int \mathrm{d}A \mathrm{Re}\left[\mathrm{i}\xi_r^{\mathrm{dyn}^*}(r,\theta,\phi) \delta P^{\mathrm{dyn}}(r,\theta,\phi) \right] \\ &= 2mr^2 \mathrm{Re}\left[\mathrm{i}\xi_r^{\mathrm{dyn}^*}(r) \delta P^{\mathrm{dyn}}(r) \right] \\ &= 2m\omega^2 \rho r^3 \mathrm{Re}\left[\mathrm{i}\xi_r^{\mathrm{dyn}^*}(r) \xi_\perp^{\mathrm{dyn}}(r) \right]. \end{aligned} \tag{22}$$

The first line in equation (22) is derived in Appendix B, and is correct to second order in the wave amplitude (cc is the complex conjugate of the first term). We have emphasized the coordinate dependence of the perturbation variables, as in equation (11), for clarity. The second line follows from averaging the first line (the angular brackets denote a time average), and the factor of 2 accounts for both the wave displacement $\boldsymbol{\xi}$ and its complex conjugate. The third line reduces the perturbations to their dynamical tide components, which we justify in Appendix B. The fourth line follows from integration over the spherical surface, and utilizes the normalization of Hough functions from equation (14). Finally, the fifth line uses the relation $\xi_\perp^{\mathrm{dyn}} \equiv \delta P^{\mathrm{dyn}}/(\rho r \omega^2)$ and shows the similarity between equation (22) and the familiar Eulerian result for non-rotating stars given by equation 39 of Paper II.

3.3 Stokes drift currents

We note that in a rotating star, the wave energy and angular momentum fluxes cannot be simply derived from the Eulerian perturbations as they are in Paper II and many other works (e.g. Lee & Saio 1993). The reasons can be traced back to the differences between Eulerian and Lagrangian averaging discussed in Andrews & McIntyre (1978a,b), and are linked with the Stokes drift terms that enter at second order in the wave amplitude. Indeed, one can naively calculate the mass flux through a spherical surface using Eulerian perturbations,

$$\begin{aligned}\dot{M}(r) &= \left\langle r^2 \int \mathrm{d}A \delta v_r(r,\theta,\phi,t)\, \delta\rho(r,\theta,\phi,t)) \right\rangle + cc \\ &= 2\omega r^2 \mathrm{Re}\left[\mathrm{i}\xi_r^*(r) \delta\rho(r) \right], \end{aligned} \tag{23}$$

which in general is non-zero, reflecting the mass transported through the surface by the Stokes drift.

One can calculate the correct second-order wave flux by subtracting out the contribution from Stokes drift. In the rotating frame, the Stokes drift velocity can be calculated from the linear wave solution via (Andrews & McIntyre 1978a)

$$\boldsymbol{v}^S = \overline{(\boldsymbol{\xi}^* \cdot \nabla)\delta\boldsymbol{v}} + cc, \tag{24}$$

where the overbar indicates an average over azimuth and time. The Stokes drift adds contributions to the wave fluxes which are implicitly included in second-order expressions such as equation (23). One can explicitly calculate the Stokes drift contribution from the Stokes drift velocity. For instance, the Stokes drift contribution to the mass flux is

$$\dot{M}^S(r) = r^2 \int \mathrm{d}A \rho v_r^S. \tag{25}$$

Some algebra shows that the mass flux of equation (23) is entirely due to the Stokes contribution of equation (25). To calculate the 'wave' contribution we simply subtract the Stokes drift contribution, therefore the mass flux due to the waves is $\dot{M}(r) = 0$ as we should expect.

We can perform a similar procedure to calculate the wave angular momentum flux from the Reynold's stress, as long as we include the torque exerted by the Coriolis force on the Stokes drift current.

[4] In our WD models, we put out outer boundary at $r = 0.99R$, below the surface convection zone, although the precise location is not important as long as it is above the radius at which the waves are excited, and in a stably stratified region where the waves roughly obey WKB scaling relations.

The end result is that the wave angular momentum flux is given by equation (22). We also note that equation (22) implies (see Appendix B) that in the rotating frame,

$$\dot{J}(r) = \frac{m}{\omega}\dot{E}(r). \tag{26}$$

This relation holds regardless of the rotation rate or the latitudinal dependence of the fluid perturbations, in accordance with Kumar, Talon & Zahn (1999).

Stokes currents are a real physical effect and are generated by propagating waves in the star. The currents cause fluid elements to drift over time, allowing them to transport mass, energy, angular momentum, metals, etc. While equation (22) accurately calculates the net tidal torque on the star, the Stokes currents may be important for the redistribution of angular momentum within the star. Additionally, a counter-current must be produced (akin to the undertow produced by breaking waves at a beach) to balance the mass transport via Stokes currents. These counter-currents are not captured by linear calculations, and they need not be equal and opposite to the Stokes drift. The Stokes drift current and counter-current may therefore set-up a circulation which could enhance mixing processes, and which could generate or reduce differential rotation. Quantifying these effects is beyond the scope of this paper, but they should be investigated in future studies.

4 TIDAL TORQUE: NUMERICAL RESULTS

We have now assembled all the ingredients necessary to calculate the tidal torque on WDs in compact binaries. Given an orbital frequency Ω and spin frequency Ω_s, the $l = |m| = 2$ component of the tidal potential has tidal forcing frequency $\omega = |2(\Omega - \Omega_s)|$ and spin parameter $q = 2\Omega_s/\omega$. We first calculate the Hough functions $H_k(q)$ for the branches k that contribute to the tidal torque, and the associated overlap integrals h_{klm} and g_{klm}. We then solve equations (20) and (21) with the outgoing wave outer boundary condition, as discussed in Paper II, and use equation (22) to calculate the associated tidal torque. In Appendix C, we discuss the inner boundary condition and subtleties that can arise when using the traditional approximation.

It is useful to express the tidal torque in dimensionless units (see Papers II and III) such that

$$T_{\rm tide} = \dot{J}_z(r_{\rm out}) = T_0 F(\omega, q), \tag{27}$$

with

$$T_0 = \frac{GM'^2}{a}\left(\frac{R}{a}\right)^5. \tag{28}$$

The quantity $F(\omega, q)$ is the dimensionless tidal torque and is related to the parametrized tidal dissipation factor Q (Goldreich & Soter 1966; Alexander 1973; Hut 1981) by $|F(\omega, q)| = 3k_2/(2Q)$, where k_2 is the tidal Love number. Note that $F > 0$ for $\Omega > \Omega_s$ and $F < 0$ for $\Omega < \Omega_s$.

Figs 3–5 show our calculations of $F(\omega, q)$ for $m = 2$ and $k = 0$ (prograde g-waves), $m = -2$ and $k = 0$ (retrograde g-waves), and $m = -2$ and $k = -2$ (retrograde r-waves), respectively. Recall that our convention for the perturbation is $e^{im\phi - i\omega t}$ with $\omega > 0$, so $m = -2$ corresponds to $\Omega < \Omega_s$, for which $F < 0$. These calculations are based on the same $M = 0.6\,M_\odot$, $T_{\rm eff} = 10^4$ K, CO WD model considered in Paper II, and the results in Fig. 3 for $q \simeq 0$ are identical to those of Paper II. The nearly vertical ridges evident in Figs 3–5 reveal the oscillatory dependence of $F(\omega, q)$ on the forcing frequency, while the increase in $F(\omega, q)$ towards larger values of ω reflects the approximate scaling $F(\omega, q) \propto \omega^5$ scaling found

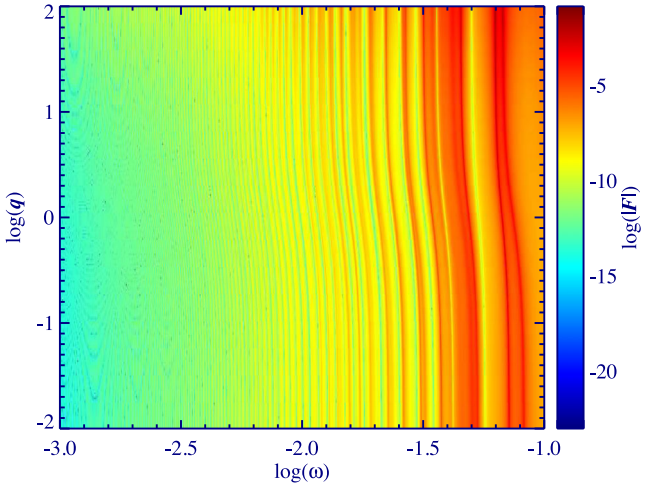

Figure 3. Dimensionless tidal torque $F(\omega, q)$ as a function of tidal forcing frequency $\omega = m(\Omega - \Omega_s)$ and rotation parameter $q = 2\Omega_s/\omega$, for the $M = 0.6\,M_\odot$, $T_{\rm eff} = 10^4$K WD model described in Paper II. This plot shows the torque exerted by the excitation of $m = 2, k = 0$ prograde g-waves responsible for tidal dissipation in subsynchronously rotating WDs. In the limit $q \to 0$, this plot is identical to the results of fig. 7 of Paper II.

in Paper II. In Figs 3 and 4, the bend in the vertical structure at $q \approx 1$ is caused primarily by the changing eigenvalue λ_k. Since the radial wavenumber for g-waves scales as $k_r^2 \simeq \lambda_k N^2/\omega^2$, the changing value of λ_k affects the radial wavelength of the tidally excited waves and thereby alters the 'resonant' forcing frequencies at which the tidal response is maximized (see Paper II).

Fig. 3 shows the tidal response for the prograde g-waves that dominate tidal spin-up for subsynchronous WDs ($\Omega > \Omega_s$). Other than the slight bend in in the resonant ridges at $q \approx 1$, the value of $F(\omega, q)$ is not strongly dependent on the value of q and hence is relatively insensitive to the rotation of the WD (as long as the WD spins subsynchronously). Consequently, the tidal torque and heating rates derived in Papers II and IV are not strongly modified by the presence of the Coriolis force, and the general conclusions of those works remain valid.

The tidal response for retrograde waves in supersynchronous WDs ($\Omega < \Omega_s$), shown in Figs 4 and 5, exhibits considerably more

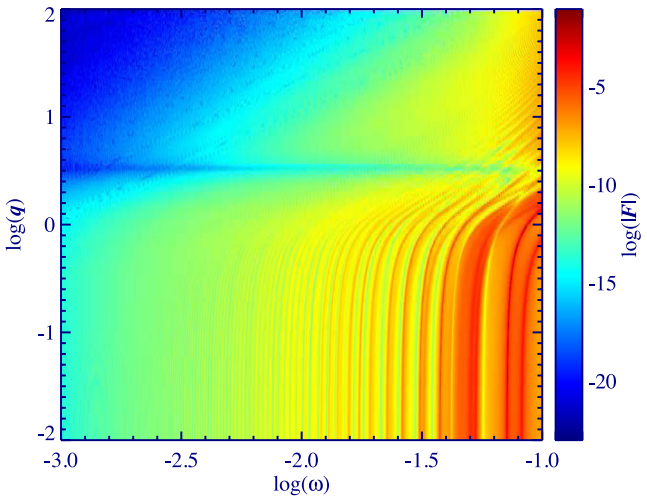

Figure 4. Same as Fig. 3, but for $m = -2, k = 0$ retrograde g-waves excited in supersynchronously rotating WDs. Note that F is negative in this case.

dependence on the value of q. The retrograde g-waves (with $k = 0$ and $m = -2$) are strongly modified by the Coriolis force, primarily because their angular eigenvalue λ_k increases rapidly for $q \gtrsim 1$ (for these waves $\lambda_k \propto q^2$ for $q \gg 1$; Bildsten et al. 1996). Not only does this cause a strong bend in the location of the resonant ridges, it also strongly reduces the tidal torque exerted by these waves. Since the value of λ_k increases with q, the radial wavelength of these waves decreases, and their overlap with the tidal potential is diminished. From equation 69 of Paper II, we find an approximate scaling $F(\omega, q) \propto \lambda_k^{-5/2} \propto q^{-5}$ for $q \gg 1$. Therefore, the retrograde g-waves provide a miniscule tidal torque at large values of q.

However, as the importance of the retrograde g-waves falls off for $q \gtrsim 1$, the $k = -2$, $m = -2$ branch of r-waves replace them and become the dominant form of tidal dissipation. Fig. 5 shows that the r-waves create a tidal response analogous to the prograde g-waves, with similar resonant ridges, and similar values of $F(\omega, q)$ (although note the different plot range in Fig. 5, as we have only plotted the region with $q > 6$ where the eigenvalue λ_k is positive). This is not too surprising, since we showed in Section 2.1 that the $k = -2$ r-waves behave like g-waves for large values of q.

Fig. 6 shows the dimensionless tidal torque $F(\omega, q)$ as a function of dimensionless orbital and spin frequency ($\bar{\Omega} = \Omega/\Omega_{\rm dyn}$, $\bar{\Omega}_{\rm s} = \Omega_{\rm s}/\Omega_{\rm dyn}$). The diagonal dark blue slice through the middle of the plot is the locus of points where spin and orbit are nearly synchronized such that $\omega < 10^{-3}\Omega_{\rm dyn}$, and lies outside of the range of our calculations. The top-left half of the plot represents supersynchronous rotation where retrograde waves cause tidal dissipation, while the bottom right represents subsynchronous rotation where prograde waves operate. The r-waves operate in the narrow slice just above the diagonal. It is evident from this plot that tidal dissipation is not symmetric across the line $\Omega = \Omega_{\rm s}$, as it would be in the absence of the Coriolis force. In the r-wave region, tidal dissipation is generally stronger than it is for the same value of $|\omega|$ corresponding to prograde g-waves, primarily because the r-waves have smaller values of λ_k and thus longer wavelengths, making them couple more effectively to the tidal potential. Conversely, in the retrograde g-wave region, where $q \approx 4$ (which appears as the blue slice above the r-wave region), neither r-waves nor g-waves are effective in generating tidal dissipation (although a precise understanding of the nature of tidal dissipation in these regions remains hampered by our use of the traditional approximation).

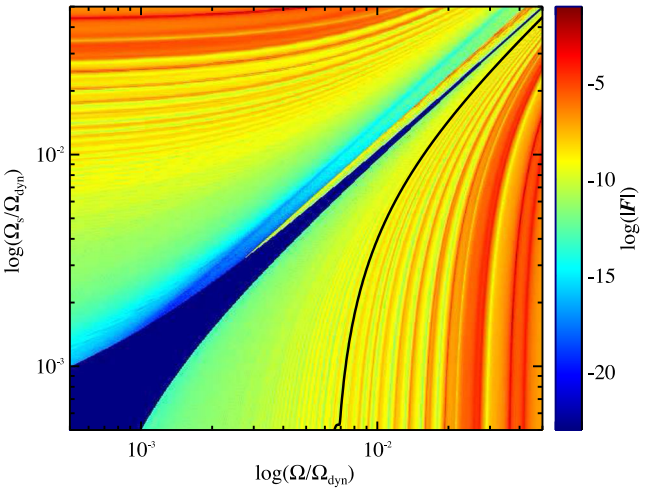

Figure 6. The dimensionless tidal torque $|F(\omega, q)|$ as a function of the orbital frequency Ω and spin frequency $\Omega_{\rm s}$. This figure shows the combined torques from Figs 3–5. The dark blue region has $\omega < 10^{-3}\Omega_{\rm dyn}$ and has not been calculated. The thick black line shows the orbital and spin evolution of an inspiraling WD binary as described in the text.

Finally, we plot the tidal torque in terms of an effective tidal Q in Fig. 7, as a function of the WD orbital period P and spin period $P_{\rm s}$. In a similar fashion to Fig. 6, the prograde g-waves occupy the upper-left part of the figure, the retrograde g-waves occupy the lower-right part, and the retrograde r-waves occupy the sliver just below the synchronization slice ($P \approx P_{\rm s}$). We can see that the effective tidal Q varies by many orders of magnitude in the parameter space investigated, and choosing a single value of Q to apply to tidal interactions in WDs is a naive procedure. Nonetheless, as discussed in Papers II and IV, the combined spin and orbital evolution of a compact WD binary may lead to a scenario in which the tidal forcing frequency ω and effective value of Q remain nearly constant as the WD orbit decays and the WD is spun up to near synchronization.

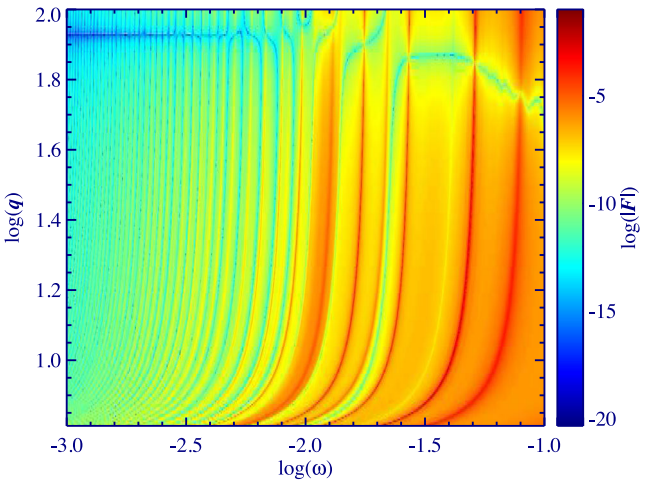

Figure 5. Same as Fig. 3, but for $m = -2, k = -2$ retrograde r-waves excited in supersynchronously rotating WDs. We have only plotted our results for $q > 6$ because the traditional approximation does not accurately characterize these r-waves for $q < 6$. Note that F is negative in this case.

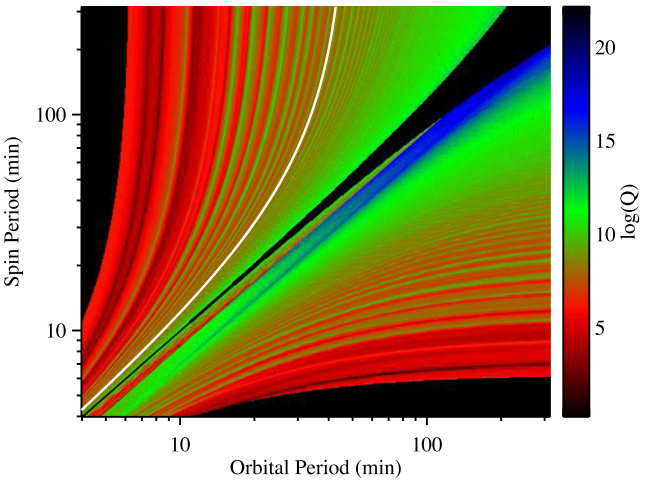

Figure 7. Tidal Q parameter of the $0.6\,{\rm M}_\odot$ WD model used in Figs 3–6, as a function of its orbital period and spin period. The black regions have $\omega > 10^{-1}\Omega_{\rm dyn}$ or $\omega < 10^{-3}\Omega_{\rm dyn}$ and have not been calculated. The thick white line shows the orbital and spin evolution of a WD binary as described in the text.

We therefore perform orbital evolution calculations similar to those of Papers II and IV, only with $F(\omega, q)$ now dependent on both ω and q. The results are shown by the black and white lines in Figs 6 and 7, for an equal mass ($M = 0.6\,M_\odot$) WD binary with no initial spin ($\Omega_s = 0$) and initial orbital period of $P = 5$ h. We find that the g-waves are indeed strongly non-linear ($\xi_r k_r > 1$) at the short orbital periods shown in Fig. 7, validating the use of the radiative outer boundary condition.[5] In a manner nearly identical to that of non-rotating WDs, the combined effects of gravitational wave-induced orbital decay and tidal spin-up act to lock the system into a state of nearly constant ω and Q at short orbital periods. Thus, the evolutionary tracks in Figs 6 and 7 trace out nearly constant values of ω, with a corresponding value of $Q \approx 10^7$.

5 DISCUSSION AND CONCLUSIONS

We have examined the effect of the Coriolis force on the excitation of dynamical tides in rotating stars, with specific application to WDs in compact binary systems. In particular, we study the dependence of the tidal dissipation on the tidal forcing frequency $\omega = m(\Omega - \Omega_s)$ and rotational parameter $q = 2\Omega_s/\omega$. We utilize the traditional approximation to examine the effect of the Coriolis force, which applies well to the gravitoinertial waves important for tidal dissipation in WDs. As one might expect, the Coriolis force is negligible when $q \ll 1$ and important when $q \gtrsim 1$.

There are four primary effects of the Coriolis force. First, it alters the angular profile of g-waves propagating in stars, changing their effective angular wavenumber λ_k and their angular overlap with the tidal potential. Secondly, the changing value of λ_k also changes the radial wavelength of the waves, modifying their radial overlap with the tidal potential. Thirdly, the Coriolis force introduces new classes of waves (inertial waves and r-waves) which rotationally mix with g-waves and provide strong tidal dissipation in certain regions of parameter space. Fourthly, the coupling of the equilibrium tidal distortion with the Coriolis force introduces new tidal forcing terms, which dominate the tidal response of the star when $q \gg 1$.

We find that the Coriolis force has a small qualitative effect on tidal dynamics in subsynchronous WDs in which prograde g-waves create most of the tidal torque. For these waves, the value of λ_k is not very dependent on q, and thus the angular and radial structure of the waves is not strongly affected. Moreover, in the traditional approximation, no prograde r-wave branches obtain positive values of λ_k, and thus there are no additional types of prograde waves that can propagate through the stably stratified interiors of WDs and cause tidal dissipation.

By contrast, the Coriolis force has a large effect on the tidal dynamics of supersynchronous WDs in which retrograde g-waves and r-waves dominate the tidal torque. The retrograde $k = 0$, $m = -2$ g-waves (which correspond to $l = 2$, $m = -2$ waves for a slowly spinning star) that dominate tidal dissipation at small values of q are strongly altered by the Coriolis force. Their angular wavenumber increases as $\lambda_k \propto q^2$, causing their radial wavelength to decrease, strongly reducing their overlap with the tidal potential and making them irrelevant for tidal dissipation when $q \gg 1$. However, the Coriolis force also introduces an r-wave branch of solutions for $q > 1$, which obtains positive λ_k for $q > 6$ (for the $k = -2$ r-waves, under the traditional approximation), leading to g-wave-like behaviour. The r-waves maintain a small but positive value of λ_k for $q \gg 1$, allowing them to couple strongly with the tidal potential and dominate tidal dissipation in this region of parameter space.

The above mentioned waves have also been identified in previous works. In the language of Pantillon, Talon & Charbonnel (2007) and Mathis et al. (2008), the prograde ($m = 2$, $k = 0$) waves are the $s = -1$ Kelvin waves (note the opposite definition of the sign of m in those works). The retrograde g-waves ($m = -2$, $k = 0$) are $s = 1$ gravitoinertial waves, and the retrograde r-waves ($m = -2$, $k = -2$) are $s = 1$ Rossby waves. The Yanai waves discussed in the above works are antisymmetric across the equator and thus not relevant to our problem, but may be relevant for tidal dissipation when the spin and orbital axes are misaligned.

It is also important to address the limitations of the traditional approximation, namely, that it does not accurately characterize the oscillation mode spectrum of a star for $q > 1$, as pointed out by Mathis et al. (2008) and examined in detail by Dintrans, Rieutord & Valdetarro (1999) and Dintrans & Rieutord (2000).[6] For $q > 1$, the oscillation equations are of a mixed hyperbolic and elliptic type, with the solutions exhibiting wave attractors such that the waves are focused on to rays where dissipation becomes very large. We have partially circumvented this problem because we consider outgoing waves which are not reflected from an outer boundary, and which cannot exhibit the periodic orbits and singularities discussed in Dintrans et al. (1999). Since the solutions we consider for $q > 1$ do not directly violate any of the assumptions of the traditional approximation (this applies to the r-wave branch so long as we consider regions with a positive eigenvalue λ_k), it appears that our results remain qualitatively and quantitatively accurate. However, we cannot rule out the possibility that additional forms of dissipation exist, e.g. due to dynamical tides composed of waves which are able to reflect near the surface of the WD and are focused on to wave attractors.

We have used our results to calculate the orbital and spin evolution of WDs in tight binary systems. Since the Coriolis force does not strongly modify the prograde g-waves that induce tidal dissipation in subsynchronously rotating inspiraling WDs, the general conclusions of Papers II–IV and Burkart et al. (2013) remain valid. Thus, compact WDs whose orbits decay via gravitational radiation should be spun up nearly to synchronization by the time Roche lobe overflow occurs, with the tidal forcing frequency ω and effective tidal Q remaining nearly constant for orbital periods less than approximately 1 h.

We can also speculate on the tidal dynamics of a WD accreting material from a companion such that the WD begins to spin supersynchronously. Our analysis indicates that the retrograde r-wave branch is capable of producing strong tidal dissipation as the WD is spun up and the tidal forcing frequency $|\omega|$ increases. Thus, we do not expect WDs accreting in compact systems (e.g. AM CVn systems) to be spun up to near breakup, as tidal dissipation will likely transfer some of the accreted angular momentum back to the

[5] At longer periods, ($P \gtrsim 45$ min), the waves are not always strongly non-linear, and may set up standing oscillation modes. In this case, the radiative outer boundary condition is not appropriate, and one must analyse g-mode excitation as discussed in Paper I and Burkart et al. (2013).

[6] Our solutions are analogous to the E_1 modes of Dintrans et al. (1999), for $q < 1$, and to the H_2 modes for $q > 1$. Similar to fig. 1c of Dintrans et al. (1999), g-waves in the traditional approximation are confined to the equatorial regions of the star. It may be possible that modes similar to the H_1 and E_2 modes of Dintrans et al. (1999) can exist near the core of the star where $N \sim 2\Omega_s$.

orbit of the donor star.[7] The spin evolution of an accreting WD in a CV system is less certain because the companion is more distant and the g-waves/r-waves may remain linear, in which case the excitation of discrete g modes studied in Paper I and Burkart et al. (2013) become important (although these discrete g modes must be modified to account for rotational effects). Whether tides can act fast enough to stabilize the mass transfer from a degenerate companion (as suggested in Nelemans et al. 2001a; Marsh et al. 2004) remains unclear, as this scenario hinges on a delicate balance of several physical mechanisms (e.g. the gravitational-wave-induced orbital decay, the mass-transfer induced orbital expansion, the tidal torque on the orbit, and the response of the donor star to mass-loss). We plan to investigate this issue in a future paper.

ACKNOWLEDGEMENTS

We thank Peter Goldreich and Rich Townsend for useful discussions. J. Fuller acknowledges partial support from NSF under grant No. AST-1205732 and through a Lee DuBridge Fellowship at Caltech. This work has been supported in part by NSF grants AST-1008245, 1211061, PHY11-25915, and NASA grants NNX12AF85G and NNX10AP19G.

REFERENCES

Alexander M. E., 1973, Astrophys. Space Sci., 23, 459
Andrews D., McIntyre M., 1978a, J. Fluid Mech., 89, 609
Andrews D., McIntyre M., 1978b, J. Fluid Mech., 89, 647
Bildsten L., Ushomirsky G., Cutler C., 1996, ApJ, 460, 827
Bloom J. et al., 2012, ApJ, 744, 17
Brown W., Kilic M., Hermes J. J., Allende Prieto C., Kenyon S. J., Winget D. E., 2011, ApJ, 737, 23
Brown W., Kilic M., Allende Prieto C., Kenyon S., 2012, ApJ, 744, 142
Burkart J., Quataert E., Arras P., Weinberg N., 2013, MNRAS, 433, 332
Chapman S., Lindzen R. S., 1970, Atmospheric Tides. Reidel, Dordrecht
Clayton G., 2012, J. Am. Var. Star Obser., 40, 539
Dall'Osso S., Rossi E. M., 2013, MNRAS, 443, 1057
Dan M., Rosswog S., Guillochon J., Ramirez-Ruiz E., 2012, MNRAS, 422, 2417
Dan M., Rosswog S., Brueggen M., Podsiadlowski P., 2013, MNRAS, 438, 14
Di Stefano R., 2010, ApJ, 719, 474
Dintrans B., Rieutord M., 2000, A&A, 354, 86
Dintrans B., Rieutord M., Valdetarro L., 1999, J. Fluid Mech., 398, 271
Fuller J., Lai D., 2011, MNRAS, 412, 1331 (Paper I)
Fuller J., Lai D., 2012a, MNRAS, 421, 426 (Paper II)
Fuller J., Lai D., 2012b, ApJ, 756, 17 (Paper III)
Fuller J., Lai D., 2013, MNRAS, 430, 274 (Paper IV)
Gilfanov M., Bogdan A., 2010, Nature, 463, 924
Goldreich P., Nicholson P., 1989a, ApJ, 342, 1075
Goldreich P., Nicholson P., 1989b, ApJ, 342, 1079
Goldreich P., Soter S., 1966, Icarus, 5, 375
Gonzalez Hernandez J., Ruiz-Lapuente P., Tabernero H. M., Montes D., Canal R., Méndez J., Bedin L. R., 2012, Nature, 489, 533
Han Z., Webbink R., 1999, A&A, 349, L17
Han Z., Podsiadlowski Ph ., Maxted P., Marsh R., Ivanova N., 2002, MNRAS, 336, 449
Heber U., 2009, ARA&A, 47, 211
Hut P., 1981, A&A, 99, 126
Iben I., Tutukov A., 1984, ApJS, 54, 335
Iben I., Tutukov A., Yungelson L., 1996, ApJ, 456, 750
Iben I., Tutukov A., Fedorova A., 1998, ApJ, 503, 344
Jeffery C., Karakas A., Saio H., 2011, MNRAS, 414, 3599
Kilic M., Brown W., Allende Prieto C., Kenyon S., Heinke C., Ageros M., Kleinman S., 2012, ApJ, 751, 141
Kilic M. et al., 2013, 438, L26
Kulkarni S. R., van Kerkwijk M. H., 2010, ApJ, 719, 1123
Kumar P., Talon S., Zahn J. P., 1999, ApJ, 520, 859
Lee U., Saio H., 1993, MNRAS, 261, 415
Lee U., Saio H., 1997, ApJ, 491, 839
Li W. et al., 2011, Nature, 480, 348
Loren-Aguilar P., Isern J., Garcia-Berro E., 2009, A&A, 500, 1193
Maoz D., Sharon K., Gal-Yam A., 2010, ApJ, 722, 1979
Marsh T., 2011, Class. Quantum. Grav., 28, 094019
Marsh T., Nelemans G., Steeghs D., 2004, MNRAS, 350, 113
Mathis S., 2009, A&A, 506, 811
Mathis S., Talon S., Pantillon F. P., Zahn J. P., 2008, Solar Phys., 251, 101
Mullally F., Badenes C., Thompson S. E., Lupton R., 2009, ApJ, 707, L51
Nelemans G., Steeghs D., Groot P., 2001a, MNRAS, 326, 621
Nelemans G., Portegies Zwart S. F., Verbunt F., Yungelson L. R., 2001b, A&A, 368, 939
Nomoto K., Kondo Y., 1991, ApJ, 367, 19
Ogilvie G. I., Lin D. N. C., 2004, ApJ, 610, 477
Pantillon F. P., Talon S., Charbonnel C., 2007, A&A, 474, 155
Piro T., 2011, ApJ, 740, L53
Raskin C., Scannapieco E., Fryer C., Rockefeller G., Timmes F., 2012, ApJ, 746, 62
Saio H., Jeffery C., 2000, MNRAS, 313, 671
Saio H., Nomoto K., 1985, A&A, 150, 21
Saio H., Nomoto K., 2004, ApJ, 615, 444
Schaefer B., Pagnotta A., 2012, Nature, 481, 164
Segretain L., Chabrier G., Mochkovitch R., 1997, ApJ, 481, 355
Steinfadt J., Kaplan D. L., Shporer A., Bildsten L., Howell S. B., 2010, ApJ, 716, L146
Townsend R. H. D., 2003, MNRAS, 340, 1020
Tutukov A., Yungelson L., 1996, MNRAS, 280, 1035
Valsecchi F., Farr W., Willems B., Kalogera V., 2012, preprint (arXiv:1210.5023)
van Kerkwijk M. H., Chang P., Justham S., 2010, ApJ, 722, 157
Warner B., 1995, Ap&SS, 225, 249
Webbink R. F., 1984, ApJ, 277, 355
Willems B., Deloye C. J., Kalogera V., 2010, ApJ, 713, 239
Yoon S.-C., Podsiadlowski Ph ., Rosswog S., 2007, MNRAS, 380, 933

[7] This statement assumes that the accreted angular momentum can be quickly transferred from the accreted layers into the core of the WD, although the precise physical mechanism and time-scale for this angular momentum transport remain unknown.

APPENDIX A: FORCED OSCILLATION EQUATIONS FOR DYNAMICAL TIDES IN ROTATING STARS

In this appendix, we derive equations (20) and (21) for the dynamical part of the tidal response of a rotating star. Although the dynamical part of the forced oscillation equations has been derived in previous studies (e.g. Paper II), the result changes considerably in a rotating star in which the latitudinal dependence of the waves is altered. The key observation is that while the equilibrium tide has a spherical harmonic angular dependence, the dynamical tide has a Hough function angular dependence. We must therefore be careful in our separation of these tidal components. We begin with the momentum equations (2)–(4):

$$-\rho\omega^2\xi_r = -\frac{\partial}{\partial r}(\delta P + \rho U) + U\frac{\partial \rho}{\partial r} - \frac{g}{c_s^2}\delta P - \rho N^2\xi_r - 2i\Omega_s\omega\rho\xi_\phi \sin\theta, \quad \text{(A1)}$$

$$-\rho\omega^2\xi_\theta = -\frac{1}{r}\frac{\partial}{\partial\theta}(\delta P + \rho U) - 2\mathrm{i}\Omega_\mathrm{s}\omega\rho\xi_\phi\cos\theta, \tag{A2}$$

$$-\rho\omega^2\xi_\phi = -\frac{1}{r\sin\theta}\frac{\partial}{\partial\phi}(\delta P + \rho U) + 2\mathrm{i}\Omega_\mathrm{s}\omega\rho\left(\xi_\theta\cos\theta + \xi_r\sin\theta\right), \tag{A3}$$

the adiabatic relation

$$\delta\rho = \frac{1}{c_\mathrm{s}^2}\delta P + \frac{\rho N^2}{g}\xi_r, \tag{A4}$$

and the continuity equation

$$\delta\rho + \frac{1}{r^2}\frac{\partial}{\partial r}\left(\rho r^2\xi_r\right) + \rho\nabla_\perp\cdot\boldsymbol{\xi}_\perp = 0. \tag{A5}$$

These equations apply for a tidally forced, spherical (non-centrifugally distorted) star in the linear and adiabatic limits, under the Cowling approximation.

The equilibrium tide is found by taking the limit $\omega \to 0$, yielding

$$\xi_r^\mathrm{eq} = -U/g, \tag{A6}$$

$$\boldsymbol{\xi}_\perp^\mathrm{eq} = -\frac{1}{l(l+1)}\nabla_\perp\frac{\partial}{\partial r}\left(\frac{Ur^2}{g}\right), \tag{A7}$$

$$\delta P^\mathrm{eq} = -\rho U, \tag{A8}$$

and here l is the component of the tidal potential (given in equations 17 and 18) we are considering. We restrict our analysis to the $l = |m| = 2$ case since these components dominate for nearly circular, aligned orbits at the orbital periods of interest.

We now let $\boldsymbol{\xi} = \boldsymbol{\xi}^\mathrm{dyn} + \boldsymbol{\xi}^\mathrm{eq}$ and $\delta P = \delta P^\mathrm{dyn} + \delta P^\mathrm{eq}$ and put these expressions into equations (A1)–(A5). We apply the traditional approximation by ignoring the ξ_ϕ^dyn term in equation (A1) and the ξ_r^dyn term in equation (A3), *but we do not drop the equilibrium tide components* since they are not negligible. After some rearranging, we find

$$\xi_r^\mathrm{dyn}\left(1 - \frac{N^2}{\omega^2}\right) = \frac{1}{\rho\omega^2}\left[\frac{\partial}{\partial r} + \frac{g}{c_\mathrm{s}^2}\right] \times\delta P^\mathrm{dyn} - \xi_r^\mathrm{eq}(r)Y_{lm} - mq\xi_\perp^\mathrm{eq}(r)Y_{lm}, \tag{A9}$$

$$\xi_\theta^\mathrm{dyn} = \frac{1}{\rho r\omega^2}\frac{1}{1-q^2\cos^2\theta}\left[\frac{\partial}{\partial\theta} - mq\frac{\cos\theta}{\sin\theta}\right]\delta P^\mathrm{dyn} - \xi_\perp^\mathrm{eq}(r)\frac{\partial}{\partial\theta}Y_{lm} + \frac{q^2\sin\theta\cos\theta}{1-q^2\cos^2\theta}\xi_r^\mathrm{eq}(r)Y_{lm}, \tag{A10}$$

$$\xi_\phi^\mathrm{dyn} = \frac{1}{\rho r\omega^2}\frac{1}{1-q^2\cos^2\theta}\left[\frac{im}{\sin\theta} - iq\cos\theta\frac{\partial}{\partial\theta}\right]\delta P^\mathrm{dyn} - \frac{im}{\sin\theta}\xi_\perp^\mathrm{eq}(r)Y_{lm} - \frac{iq\sin\theta}{1-q^2\cos^2\theta}\xi_r^\mathrm{eq}(r)Y_{lm}, \tag{A11}$$

$$\delta P^\mathrm{dyn} = \rho g\xi_r^\mathrm{dyn} - \frac{\rho c_\mathrm{s}^2}{r^2}\frac{\partial}{\partial r}\left(r^2\xi_r^\mathrm{dyn}\right) - \rho c_\mathrm{s}^2\nabla_\perp\cdot\boldsymbol{\xi}_\perp^\mathrm{dyn}. \tag{A12}$$

Here, we have explicitly expressed the angular dependence of the equilibrium tide terms in terms of spherical harmonics, and defined

$$\xi_\perp^\mathrm{eq}(r) = -\frac{1}{l(l+1)r}\frac{\partial}{\partial r}\left[\frac{U(r)r^2}{g}\right]. \tag{A13}$$

equations (A9)–(A11) show that we can think of the dynamical tide as being forced by the equilibrium tidal distortion rather than by the tidal potential. Note that the last term in equations (A9)–(A11) are additional tidal forcing terms that vanish in the limit $q \to 0$. The spin frequency Ω_s does not explicitly appear in equations (A9)–(A11) because we have used $2\Omega_\mathrm{s} = q\omega$.

Substituting equations (A10) and (A11) into equation (A12), we obtain

$$\delta P^\mathrm{dyn} = \rho g\xi_r^\mathrm{dyn} - \frac{\rho c_\mathrm{s}^2}{r^2}\frac{\partial}{\partial r}\left(r^2\xi_r^\mathrm{dyn}\right) - \rho c_\mathrm{s}^2\left[\frac{1}{\rho r^2\omega^2}\mathcal{L}\,\delta P^\mathrm{dyn} + \frac{l(l+1)}{r}\xi_\perp^\mathrm{eq}Y_{lm} - \frac{q^2}{r}\xi_r^\mathrm{eq}\frac{\partial}{\partial\mu}\left(\frac{1}{1-q^2\mu^2}\mu(1-\mu^2)Y_{lm}\right) + \frac{qm}{r}\xi_r^\mathrm{eq}\frac{1}{1-q^2\mu^2}Y_{lm}\right]. \tag{A14}$$

Here, $\mathcal{L}$ is the Laplace tidal operator from equation (9), and $\mu = \cos\theta$. We now decompose the dynamical tide into Hough functions H_k, and integrate equations (A9) and (A14) over a spherical surface to obtain

$$\xi_r^\mathrm{dyn}\left(1 - \frac{N^2}{\omega^2}\right) = \frac{1}{\rho\omega^2}\left[\frac{\partial}{\partial r} + \frac{g}{c_\mathrm{s}^2}\right]\delta P^\mathrm{dyn} - h_{klm}\left(\xi_r^\mathrm{eq} + mq\xi_\perp^\mathrm{eq}\right), \tag{A15}$$

and

$$\delta P^\mathrm{dyn}\left(1 - \frac{\lambda_k c_\mathrm{s}^2}{r^2\omega^2}\right) = \frac{\rho c_\mathrm{s}^2}{r^2}\left[\frac{g}{c_\mathrm{s}^2} - \frac{\partial}{\partial r}\right]\left(r^2\xi_r^\mathrm{dyn}\right) - \rho c_\mathrm{s}^2\left[\frac{l(l+1)h_{klm}}{r}\xi_\perp^\mathrm{eq} + \frac{g_{klm}}{r}\xi_r^\mathrm{eq}\right]. \tag{A16}$$

The angular overlap integrals h_{klm} and g_{klm} describe the angular coupling with the tidal potential and are given by

$$h_{klm} = \int \mathrm{d}A\, Y_{lm}H_k\mathrm{e}^{-\mathrm{i}m\phi} \tag{A17}$$

and

$$\begin{aligned} g_{klm} &= q^2\int\mathrm{d}A\frac{1}{\sin\theta}\frac{\partial}{\partial\theta}\left(\frac{\sin^2\theta\cos\theta}{1-q^2\cos^2\theta}Y_{lm}\right)H_k\mathrm{e}^{-\mathrm{i}m\phi} + qm\int\mathrm{d}A\frac{1}{1-q^2\cos^2\theta}Y_{lm}H_k\mathrm{e}^{-\mathrm{i}m\phi} \\ &= -q^2\int\mathrm{d}A\left(\frac{\sin\theta\cos\theta}{1-q^2\cos^2\theta}Y_{lm}\right)\frac{\partial}{\partial\theta}H_k\mathrm{e}^{-\mathrm{i}m\phi} + qm\int\mathrm{d}A\frac{1}{1-q^2\cos^2\theta}Y_{lm}H_k\mathrm{e}^{-\mathrm{i}m\phi} \\ &= \mathrm{i}q\int\mathrm{d}A\sin\theta\xi_r^\mathrm{eq}(\theta,\phi)\xi_\phi^{\mathrm{dyn}^*}(\theta,\phi), \end{aligned} \tag{A18}$$

with the second equality following from integrating the first term by parts. In the third equality, we have used definitions $\xi_r^\mathrm{eq}(\theta,\phi) = Y_{lm}(\theta,\phi)$ and $\xi_\phi^{\mathrm{dyn}^*}(\theta,\phi)$ given by the angular part of the right-hand side of equation (13) to highlight the origin of the angular integral composing g_{klm}. Equations (A15) and (A16) are identical to equations (20) and (21) and can be numerically integrated to find the dynamical component of the tidal response. The last terms in equations (A15) and (A16) vanish for a non-rotating star, and do

not appear if one mistakenly applies the traditional approximation to the equilibrium component of the tidal response. For $q \gg 1$, these terms dominate the tidal forcing, and so they must be included.

APPENDIX B: ANGULAR MOMENTUM FLUX IN ROTATING STARS

B1 Angular momentum flux through a surface

In this appendix, we provide a simple derivation of the angular momentum flux through the quasi-spheriodal surface of a perturbed spherical shell. The derivation is simplest if we adopt an inertial frame of reference. We begin from the z-component of the angular momentum equation:

$$\frac{\partial}{\partial t} j_z + \nabla \cdot \left(j_z \boldsymbol{v} \right) = -\frac{\partial}{\partial \phi} P - \rho \frac{\partial}{\partial \phi} U, \tag{B1}$$

where $j_z = \rho r \sin\theta v_\phi$ is the z-component of the angular momentum density. We integrate equation (B1) over the perturbed volume $\tilde{V}$ corresponding to the spherical shell initially at radius r in the unperturbed star. With the Reynold's transport theorem this yields

$$\frac{\mathrm{d}}{\mathrm{d}t} \int \mathrm{d}\tilde{V} j_z = -\int \mathrm{d}\tilde{V} \frac{\partial}{\partial \phi} P - \int \mathrm{d}\tilde{V} \rho \frac{\partial}{\partial \phi} U. \tag{B2}$$

Note that the perturbed volume $\mathrm{d}\tilde{V}$ can be expressed as the unperturbed volume $\mathrm{d}V$ plus a surface perturbation, i.e. $\mathrm{d}\tilde{V} = \mathrm{d}V + r^2 \xi_r \mathrm{d}A$, where $\mathrm{d}A$ is the solid angle element. Then equation (B2) becomes, to second order in perturbation amplitude,

$$\frac{\mathrm{d}}{\mathrm{d}t} J_z = -r^2 \int \mathrm{d}A \xi_r \frac{\partial}{\partial \phi} \left(\delta P + \rho U \right) - \int \mathrm{d}V \delta\rho \frac{\partial}{\partial \phi} U, \tag{B3}$$

where we have ignored first-order terms that time average to zero. The left-hand side of equation (B3) is the time derivative of the total angular momentum $J_z = \int \mathrm{d}\tilde{V} j_z$, while the first term on the right-hand side is the angular momentum flux term given in equation (22) and the last term is the torque from the tidal potential. The time derivative of the angular momentum of any fluid element is zero if there is no wave dissipation within the volume (Goldreich & Nicholson 1989a,b) as shown explicitly in Section B3. Since the wave dissipation occurs outside of our integration region, the terms on the right-hand side of equation (B3) exactly cancel each other out. The torque is identical in the rotating and non-rotating frames, and so the flux term in equation (B3) can be applied in the rotating frame (so long as the change in wave frequency is taken into account). Equation (B3) can also be derived in the rotating frame, although the derivation is more complex because torques from the Coriolis force must be included.

It is also instructive to derive the energy flux through a comoving fluid surface. In the rotating frame, we have

$$\frac{\mathrm{d}}{\mathrm{d}t} \int \mathrm{d}\tilde{V} \varepsilon = -\int \mathrm{d}\tilde{V} \rho \nabla\Phi \cdot \boldsymbol{v} - \int P \boldsymbol{v} \cdot \mathrm{d}\tilde{\boldsymbol{S}}, \tag{B4}$$

where ε is the energy density, Φ is the total gravitational potential, and $\tilde{\boldsymbol{S}}$ is the perturbed surface element. To second order

$$\frac{\mathrm{d}}{\mathrm{d}t} \int \mathrm{d}\tilde{V} \varepsilon = -\int \mathrm{d}V g \, \delta\rho \, \delta v_r - \int \mathrm{d}V \rho \nabla U \cdot \delta\boldsymbol{v} - r^2 \int \mathrm{d}A \, \delta P \, \delta v_r. \tag{B5}$$

The term proportional to g must vanish because the surface integral $\int \mathrm{d}A \, \delta\rho \, \delta v_r$ must vanish in order to conserve mass.[8] We transform the second term by noting that

$$\int \mathrm{d}V \rho \nabla U \cdot \delta\boldsymbol{v} = \int \mathrm{d}V \nabla \cdot (\rho U \delta\boldsymbol{v}) - \int \mathrm{d}V U \nabla \cdot (\rho \delta\boldsymbol{v}) = r^2 \int \mathrm{d}A \rho U \delta v_r + \int \mathrm{d}V U \frac{\partial}{\partial t} \delta\rho, \tag{B6}$$

where the terms in the second line arise from applying Gauss's theorem and the continuity equation, respectively. We then have

$$\frac{\mathrm{d}}{\mathrm{d}t} E = -r^2 \int \mathrm{d}A \left(\delta P + \rho U \right) \delta v_r - \int \mathrm{d}V U \frac{\partial}{\partial t} \delta\rho. \tag{B7}$$

The first term on the right-hand side is the energy flux out of the surface, while the second is the work done by the tidal potential. Recalling that $\delta v_r = -\mathrm{i}\omega\xi_r$, it is evident that the energy flux and angular momentum flux are related by $\dot{J}_z = m\dot{E}/\omega$.

B2 Comparison to previous results

We comment on the expressions for angular momentum flux used in previous works such as Pantillon et al. (2007) and Mathis (2009). These works quote the z-component of the angular momentum flux as

$$\dot{J}_z = \int \mathrm{d}A \rho r^3 \left[\sin\theta \delta v_r \delta v_\phi + 2 \sin\theta \cos\theta \Omega_\mathrm{s} \xi_r \delta v_\theta \right] = \frac{2m'}{\omega} \dot{E}_k, \tag{B8}$$

where m' is a numerically calculated effective azimuthal wavenumber that depends on the stellar spin frequency and $\dot{E}_k$ is the kinetic energy flux carried by the wave.

Equation (B8) can be somewhat reconciled with equations (22) and (26). We note that equation (4) can be written as

$$\rho r \left(-\mathrm{i}\omega \sin\theta \delta v_\phi + 2 \sin\theta \cos\theta \Omega_\mathrm{s} \delta v_\theta \right) = -\frac{\partial}{\partial \phi} \left(\delta P + \rho U \right) - 2\rho r \sin^2\theta \Omega_\mathrm{s} \delta v_r. \tag{B9}$$

Multiplying by ξ_r yields

$$\rho r \left(\sin\theta \delta v_r \delta v_\phi + 2 \sin\theta \cos\theta \Omega_\mathrm{s} \xi_r \delta v_\theta \right) = -\xi_r \frac{\partial}{\partial \phi} \left(\delta P + \rho U \right) - 2\rho r \sin^2\theta \Omega_\mathrm{s} \xi_r \delta v_r. \tag{B10}$$

The last term on the right-hand side vanishes upon addition of its complex conjugate. Then we have

$$\dot{J}_z = -r^2 \int \mathrm{d}A \xi_r \frac{\partial}{\partial \phi} \left(\delta P + \rho U \right) = \frac{m}{\omega} \dot{E}, \tag{B11}$$

in accordance with equations (22) and (26). Thus, it is not necessary to numerically calculate the angular integral m', and the energy and angular momentum fluxes are always related by a factor of m as long as the unperturbed stellar structure is axisymmetric. The factor

[8] This term must vanish to conserve mass, although, as pointed out in the text, it does not vanish until one includes the effect of a current that develops to counteract the Stokes drift current. Here we assume that such a current is indeed present, conserving mass and cancelling the gravitational potential energy flux term of equation (B5).

of 2 difference between the energy flux in equations (B11) and (B8) arises because equation (B8) refers only to the kinetic energy flux of the wave, $\dot{E}_k$, which is related to the total energy (kinetic and potential) flux by $\dot{E} = 2\dot{E}_k$.

The conclusions above are independent of the traditional approximation, although one may reach the same conclusion by manipulating equations (12) and (13). From equation (B8), using the traditional approximation, we have

$$\begin{aligned}
\dot{J}_z &= \int \mathrm{d}A\rho r^3 \left[\sin\theta \delta v_r \delta v_\phi + 2\sin\theta\cos\theta\Omega_s \xi_r \delta v_\theta\right] \\
&= 2\omega^2 \int \mathrm{d}A\rho r^3 \left[\sin\theta \mathrm{Re}\left(\xi_r^* \xi_\phi\right) + q\sin\theta\cos\theta \mathrm{Re}\left(\mathrm{i}\xi_r^* \xi_\theta\right)\right] \\
&= 2\omega^2 \int \mathrm{d}A\rho r^3 \mathrm{Re}\left[\xi_r^* \left(\frac{\sin\theta}{1-q^2\cos^2\theta}\left[\frac{\mathrm{i}m}{\sin\theta} - \mathrm{i}q\cos\theta\frac{\partial}{\partial\theta}\right]\xi_\perp \right.\right. \\
&\quad \left.\left. + \frac{\mathrm{i}q\sin\theta\cos\theta}{1-q^2\cos^2\theta}\left[\frac{\partial}{\partial\theta} - mq\frac{\cos\theta}{\sin\theta}\right]\xi_\perp\right)\right] \\
&= 2\omega^2 \int \mathrm{d}A\rho r^3 \mathrm{Re}\left[\frac{1}{1-q^2\cos^2\theta}\xi_r^* \left(\mathrm{i}m\left[1-q^2\cos^2\theta\right]\right)\xi_\perp\right] \\
&= 2m\omega^2\rho r^3 \mathrm{Re}\left[\mathrm{i}\xi_r^* \xi_\perp\right]. \qquad \text{(B12)}
\end{aligned}$$

The second line follows from $2\Omega_s = \omega q$ and using $\delta\boldsymbol{v} = -\mathrm{i}\omega\boldsymbol{\xi}$, the third from equations (12) and (13), the fourth from combination of terms, and the fifth from angular integration over a sphere. Thus, the traditional approximation obeys the angular momentum flux and energy flux relation of equation (26).

Some previous authors (e.g. Lee & Saio 1993) have obtained an additional angular momentum flux term,

$$\dot{J}_{z,\rho} = \Omega_s r^4 \int \mathrm{d}A \sin^2\theta\, \delta\rho\, \delta v_r. \qquad \text{(B13)}$$

This term does not actually contribute to angular momentum transfer via waves. It vanishes upon subtraction of terms due to Stokes drift velocities, as described in Section 3.3. Regardless, in WD interiors the angular momentum flux from equation (B13) is small compared to that of equation (22) because $|\delta\rho/\rho| \ll |\xi_\perp/r|$ for gravity waves in the WKB limit.

B3 Deposition of angular momentum

In this section, we show explicitly how the angular momentum of a shell of thickness dr evolves with time. In particular, we show that in the absence of local wave dissipation, there is no net torque on the shell.

The amount of angular momentum deposited in a shell of thickness dr due to the change in angular momentum flux across it is

$$\begin{aligned}
\frac{\partial}{\partial t}4\pi r^2 j_z(r)\mathrm{d}r &= \mathrm{d}r\frac{\partial}{\partial r}\dot{J}_z(r) \\
&= 2\mathrm{d}r\frac{\partial}{\partial r}\int \mathrm{d}A\,\mathrm{Re}\left[r^2\xi_r^*(r,\theta,\phi)\right. \\
&\quad \left.\times\frac{\partial}{\partial\phi}\left(\delta P(r,\theta,\phi) + \rho U(r,\theta,\phi)\right)\right] \\
&= 2m\mathrm{d}r\int \mathrm{d}A\mathrm{Re}\left[\mathrm{i}\left(\delta P(r,\theta,\phi) + \rho U(r,\theta,\phi)\right)\right. \\
&\quad \left.\times\frac{\partial}{\partial r}\left(r^2\xi_r^*(r,\theta,\phi)\right)\right] \\
&\quad + 2m\mathrm{d}r\int \mathrm{d}A\,\mathrm{Re}\left[\mathrm{i}\left(r^2\xi_r^*(r,\theta,\phi)\right)\right. \\
&\quad \left.\times\frac{\partial}{\partial r}\left(\delta P(r,\theta,\phi) + \rho U(r,\theta,\phi)\right)\right], \qquad \text{(B14)}
\end{aligned}$$

with the second line following by inserting equation (22). To evaluate the radial derivatives, we use equations (2) and (6), along with the adiabatic relation of equation (5) to find

$$\begin{aligned}
\frac{\partial}{\partial t}4\pi r^2 j_z(r)\mathrm{d}r &= 2m\mathrm{d}r\int \mathrm{d}A\,\mathrm{Re}\left[-\mathrm{i}r^2 U\delta\rho^* - \mathrm{i}r^2\left(\delta P + \rho U\right)\right. \\
&\quad \left.\times\nabla_\perp\cdot\boldsymbol{\xi}_\perp^* + 2\Omega_s\omega\rho r^2\sin\theta\xi_r^*\xi_\phi\right] \\
&= 2m\mathrm{d}r\int \mathrm{d}A\mathrm{Re}\left[-\mathrm{i}r^2 U\delta\rho^* - \nabla_\perp\cdot\right. \\
&\quad \left[\mathrm{i}r^2\left(\delta P + \rho U\right)\boldsymbol{\xi}_\perp^*\right] + \boldsymbol{\xi}_\perp^*\cdot\nabla_\perp \\
&\quad \left.\times\left[\mathrm{i}r^2\left(\delta P + \rho U\right)\right] + 2\Omega_s\omega\rho r^2\sin\theta\xi_r^*\xi_\phi\right] \\
&= 2m\mathrm{d}r\int \mathrm{d}A\mathrm{Re}\left[-\mathrm{i}r^2 U\delta\rho^* - 2\Omega_s\omega\rho r^2\cos\theta\right. \\
&\quad \times\left(\xi_\theta\xi_\phi^* - \xi_\theta\xi_\phi^*\right) - 2\Omega_s\omega\rho r^2\cos\theta \\
&\quad \left.\times\left(\xi_r\xi_\phi^* - \xi_r^*\xi_\phi\right)\right] \\
&= 2m\mathrm{d}r\int \mathrm{d}A\,\mathrm{Re}\left[-\mathrm{i}r^2 U\delta\rho^*\right]. \qquad \text{(B15)}
\end{aligned}$$

The second line arises from rearranging the horizontal divergence term. The surface integral of a horizontal divergence vanishes on a closed surface, eliminating the second term on the second line, and inserting equations (3) and (4) we obtain the third line. The terms in parentheses are purely imaginary, leaving us with the simple result of the fourth line.

The fourth line of equation (B15) is equal to the negative of the torque exerted on the shell by the tidal potential. Therefore, in the absence of local non-adiabatic effects, the angular momentum of any region of the star remains unchanged by tidal torques and wave propagation, as proven more generally in Golreich & Nicholson (1989a). Basically, in the absence of dissipation, any angular momentum deposited in a region via tidal torques is transported away by the waves.

This fact can help us understand why we need to only calculate the dynamical tide contributions to equation (22). Although the equilibrium tide–dynamical tide cross-terms contribute to the angular momentum flux, they are exactly cancelled by torques from the tidal potential. The terms due purely to dynamical tide cannot be ignored because, away from the regions of excitation or damping, their angular momentum luminosity remains constant (and therefore do not contribute to equation B15). This assertion is easily verified in the WKB limit (see Paper II). To calculate the total angular momentum luminosity flowing into the outer regions of the star,

one could either evaluate the surface integral of equation (22), or the volume integral of equation (B3). However, since the integrand of the last term equation (B3) is highly oscillatory with radius, a volume integral is highly susceptible to numerical errors, and we find it much easier to use the last line of equation (22).

APPENDIX C: INNER BOUNDARY CONDITION

The traditional approximation encounters problems at the centre of the star, where $r \to 0$ because both postulates of the approximation are broken (near the centre of the star $N \to 0$ and $\xi_r \approx \xi_\theta$). As we will see below, the manifestation of these problems is the divergence of the dynamical tide solution at the centre of the star, which is obviously unphysical.

The oscillation equations (20) and (21) take the form at the centre of the star (where $r \to 0$, $\rho \to \rho_c$, $g \to 4\pi G\rho_c r/3$, and $\partial g/\partial r \to 4\pi G\rho_c/3$, with ρ_c the central density):

$$\frac{\partial}{\partial r}\delta P^{\rm dyn} \simeq \rho\omega^2\xi_r^{\rm dyn} + h_{klm}\rho\omega^2\xi_r^{\rm eq} + h_{klm}mq\rho\omega^2\xi_\perp^{\rm eq}, \tag{C1}$$

$$\frac{\partial}{\partial r}\xi_r^{\rm dyn} \simeq -\frac{2}{r}\xi_r^{\rm dyn} + \frac{\lambda_k}{\rho r^2\omega^2}\delta P^{\rm dyn} - \frac{h_{klm}l(l+1)}{r}\xi_\perp^{\rm eq} - \frac{g_{klm}}{r}\xi_r^{\rm eq}. \tag{C2}$$

Imposing a Frobenius expansion such that $\xi_r^{\rm dyn} \propto r^\alpha$, $\delta P^{\rm dyn} \propto r^{\alpha+1}$, and defining $U_c = -\frac{3M'W_{22}}{4\pi\rho_c a^{l+1}}$, we have

$$\frac{\alpha+1}{\rho r\omega^2}\delta P^{\rm dyn} \simeq \xi_r^{\rm dyn} + h_{klm}U_c r^{l-1} + \frac{h_{klm}mq}{l}U_c r^{l-1}, \tag{C3}$$

$$\frac{\alpha+2}{r}\xi_r^{\rm dyn} \simeq \frac{\lambda_k}{\rho r^2\omega^2}\delta P^{\rm dyn} - (l+1)h_{klm}U_c r^{l-2} - g_{klm}U_c r^{l-2}. \tag{C4}$$

These equations have both particular (forced) solutions and homogeneous (free) solutions. The forced solutions have $\xi_r^{\rm dyn} \propto r^{l-1}$ and thus vanish near the origin. The free solution satisfies

$$\frac{\alpha+1}{\rho r\omega^2}\delta P^{\rm dyn} \simeq \xi_r^{\rm dyn}, \tag{C5}$$

$$\frac{\alpha+2}{r}\xi_r^{\rm dyn} \simeq \frac{\lambda_k}{\rho r^2\omega^2}\delta P^{\rm dyn}, \tag{C6}$$

which requires

$$\alpha^2 + 3\alpha + (2-\lambda_k) = 0. \tag{C7}$$

The solutions of this quadratic equation are

$$\alpha = -\frac{3}{2} \pm \frac{1}{2}\sqrt{9 + 4(\lambda_k - 2)}. \tag{C8}$$

If $\lambda_k > 2$, there exists a regular solution with $\alpha > 0$, allowing one to set $\xi_r^{\rm dyn} = \delta P^{\rm dyn} = 0$ at $r = 0$. However, if $\lambda_k < 2$ there is no solution for which $\alpha > 0$, and thus there exists no regular solution at $r = 0$. Any solution of equations (20) and (21) for $\lambda_k < 2$ therefore diverges near the origin.

As stated above, this unphysical divergence can be attributed to the breakdown of the traditional approximation near the origin. This issue is especially worrisome for the $k = -2$, $m = -2$ r-waves for which $\lambda_k < 2$ for all values of q. In practice, when computing a solution with $\lambda_k < 2$, we choose the positive solution of equation (C8) and use for our inner boundary condition the relation

$$\rho r_{\rm in}\omega^2\xi_r^{\rm dyn} = (\alpha+1)\delta P^{\rm dyn}, \tag{C9}$$

computed at some very small vale of $r_{\rm in}$. We find that the choice of $r_{\rm in}$ does not affect the solution near the outer boundary, nor does it affect computed values of $F(\omega, q)$. Although this method cannot be used to characterize the dynamical tide solution near the origin, we conclude that it yields accurate solutions away from the origin where the traditional approximation is valid.

This paper has been typeset from a TEX/LATEX file prepared by the author.